Conference Paper

Analysis of Surface Orange Peel of Automotive Aluminum Alloy Pipe Using Electron Backscatter Diffraction (EBSD)

D.Y. Chao[1], W.Z. Shao[1,2], J.T. Jiang[1,2], and L. Zhen[1]

[1]School of Materials Science and Engineering, Harbin Institute of Technology, Harbin 150001, China
[2]National Key Laboratory of Precision Hot Processing of Metals, Harbin Institute of Technology, Harbin 150001, China

Abstract

The occurrence of orange peel in 6xxx alloy tube for automotive application was studied by super depth metallographic microscope and EBSD. The results revealed obvious ups and downs morphology at the surface after tube hydroforming. Compared with the undeformed case, more grains existed in the concave areas rather than individual out-of-plane displacement. The influence of surface orange peel on grain boundary morphology, crystal orientation, and texture are discussed. It is concluded, that surface orange peel is controlled by the spatial distribution of grain orientations and grain size through the thickness of the sample.

Keywords: tube hydroforming; orange peel; EBSD; grains orientation

Corresponding Author: W.Z. Shao; email: wzshao@hit.edu.cn

Received: 9 September 2016
Accepted: 19 September 2016
Published: 12 October 2016

Publishing services provided by Knowledge E

Selection and Peer-review under the responsibility of the ASRTU Conference Committee.

OPEN ACCESS

1. Introduction

Due to the requirements for weight reduction in automotive, Al-Mg-Si alloys are increasingly used in automotive structural applications owing to their combination of high strength, low density, and good formability [1, 2]. At the same time, the surface defects appear during the fabrication of sheet and tube productions [3-5]. A common defect of roping or ridging has been extensively investigated by rolling and tensile deformation. More studies have been focused on the origin of surface defects and on quantitative estimation of dependence of associated surface roughening on the spatial gain orientation distribution using the technique of electron backscatter diffraction (EBSD) [3, 4]. A clear relationship between roping development and the spatial distribution of the Goss component was identified [6]. Orange peel as a mesoscale roughing existing in the sheet and tube metal deformations can affect surface quality of tamping and bulging parts. Previous work pointed out, that orange peel phenomena took place as the crystals underwent individual out-of-plane displacements at the surface. No clear relationship with the crystallographic orientation of the surface grains was established [5, 7]. Nevertheless, Cao pointed out that the coarse grains with {100}<001> micotexture formed bulging and yielded orange peel defects of the steel sheet [8]. While it was detected, that the orange peel often occurred at the

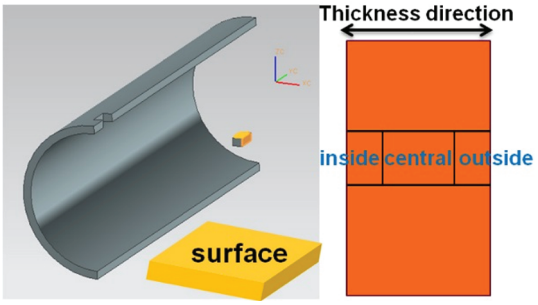

Figure 1: Schematic representations of surface and thickness direction.

surface during tube hydroforming process due to the load path, this fact was often overlooked.

(EBSD has become a common technique that provides the imaging of microstructures, crystallographic orientation of grains, and their spatial distribution over a large specimen area. It has been revealed by EBSD technique that spatial distribution of grain orientation through the thickness is responsible for the surface roughening [4]. In this article, we describe the surface morphology, grain boundaries, and orientation maps at the tube surface during tube hydroforming process as well as along thickness direction. The study is aimed at establishing the relationship between the grain morphology, grain angle boundaries, and grain orientation at the surface as well as along thickness direction with the orange peel phenomena. However, the mechanism of formation of the orange peer remains unclear and further studies are needed [1, 2].

2. Methods

The 6063 aluminum alloy selected for presented study was developed primarily for automotive applications. The outer diameter of the tube is 78 mm and the thickness is 4 mm. The ultimate tensile strength, yield strength, and elongation for the 6063-T4 sample are 187.5 MPa, 86.97 MPa, and 24.38%, respectively. The bursting occurs at the center of the wrinkle wave of tube hydroforming. The samples were cut from tow areas as shown in Fig. 1: (i) the surface of the tube before deformation and the edge of rupture area with the serious areas of orange peel after tube hydroforming; (ii) three areas of the outer, center, and inside along the thickness direction. The macro-morphology of the surface was observed by super depth metallographic microscope (VHX-1000E). Samples for EBSD measurement were mechanically polished followed by electro-polishing using 5% perchloric acid in alcohol. The samples were examined using scanning electron microscopy (Quanta 200FEG) equipped with EBSD. Two types of maps were derived from EBSD analysis: grains boundary maps and crystal orientation map. On the obtained boundary maps the blue, green, and red lines are high angle boundaries with misorientation angle above 15°, low angle boundaries with angles ranging from 5° to 15° and the boundaries with misorientation angles from 2° to 5°, respectively.

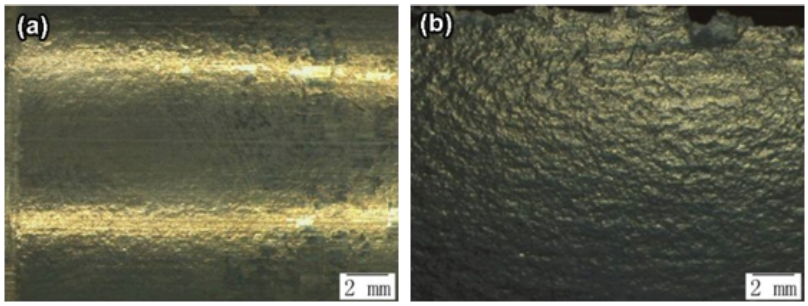

Figure 2: Surface morphology of the tube: (a) before deformation and (b) after tube hydroforming.

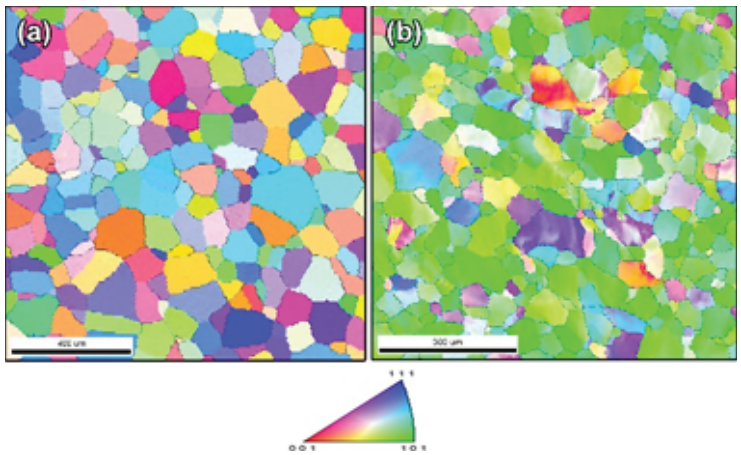

Figure 3: Crystal orientation map in inverse-pole-figure coloring of the surface samples: (a) before deformation and (b) after tube hydroforming.

3. Results

Fig. 2 shows the surface morphology of the tube before and after its hydroforming. Prior to deformation, a smooth surface morphology of the tube is presented in Fig. 2a. The pronounced ups and downs called orange peel found at the edge of rupture area are shown in Fig. 2b. All the samples were cut from the two areas for further analysis by EBSD of the cause of formation of the orange peel defects.

The crystal orientation maps in inverse-pole-figure coloring of the surface with respect to the axis of the tube are shown in Fig. 3. The color key indicates the grain orientation. As it is seen the grains demonstrated random orientation distribution before deformation (Fig. 3a). A slight tendency toward to the <101> orientation can be found after tube hydroforming as shown in Fig. 3b. Additionally, the normal orientation maps analysis performed with EBSD indicated that the average grain size at the surface was about 120 μm (Fig. 3a).

Fig. 4 presents the grain boundary maps at the surface of the samples, showing the evolution on the surface morphology during hydro-bugling. Fig. 4a demonstrates the well-known fact that most grain boundaries at the tube surface are high angle boundaries with the misorientation angles >15°. However, the number of grains boundaries with low angle boundaries (angles <15°) increased during tube hydroforming. This indicates that the nonuniform deformation exists in these areas, as shown in Fig.

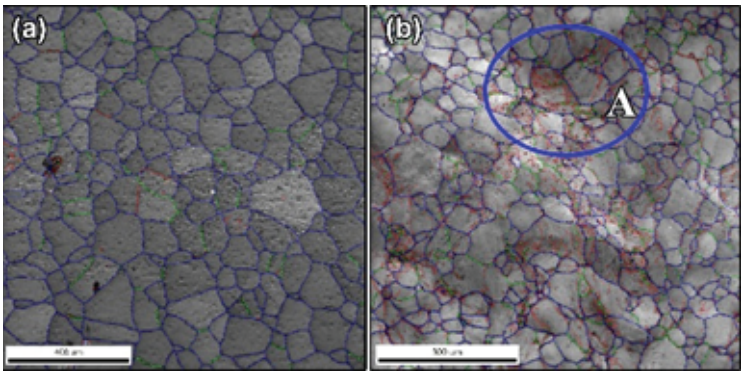

Figure 4: Grain boundary maps from EBSD date of the samples: (a) before deformation and (b) after tube hydroforming.

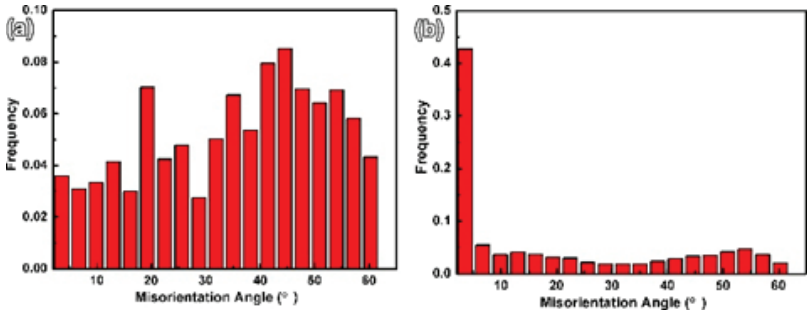

Figure 5: Misorientation angle distribution of the grain boundaries of the samples: (a) before deformation and (b) after tube hydroforming.

4b. The pronounced concave-convex uneven surface morphology is observed in the grain boundary map. In the concave areas (A area), a number of grains with low angle boundaries, but not individual out-of-plane displacements, were registered [5]. In addition, the morphology of orange peel resulting from anisotropy of tube hydroforming is inconsistent with the anisotropy of plastic strain inside grains. By analysis of the angle misorientation in the studied sample area using EBSD data, the crystallographic orientation of all grains can be determined, which makes possible to calculate the misorientation between neighboring grains [3]. Fig. 5 shows the misorientation angle distribution of the grain boundaries in the sample. Prior to deformation (as shown in Fig. 5a), the distribution of misorientation angles concentrates mainly within the high angle range and the average misorientation angle is 35.4°. The distribution of misorientation angles in the orange peel area extends to low angles range (the angles <15°), as shown in Fig. 5b.

The variation trend of the grain characteristic along the thickness direction can provide better understanding of orange peel arising at the surface after tube hydroforming. Fig. 6 shows the dependence of grain boundaries distribution and orientation maps obtained from EBSD date on the thickness in the undeformed tube. The high angle boundaries with the angles exceeding 15° along the thickness direction play the dominant role in the three areas, which corresponds to the results shown in Fig. 4a. We have also found that the grain size in the central area is smaller than in the other areas. The random orientation distribution of the grains is observed in these areas, especially at the edge regions of the outside and inside areas. The non-uniform distribution of

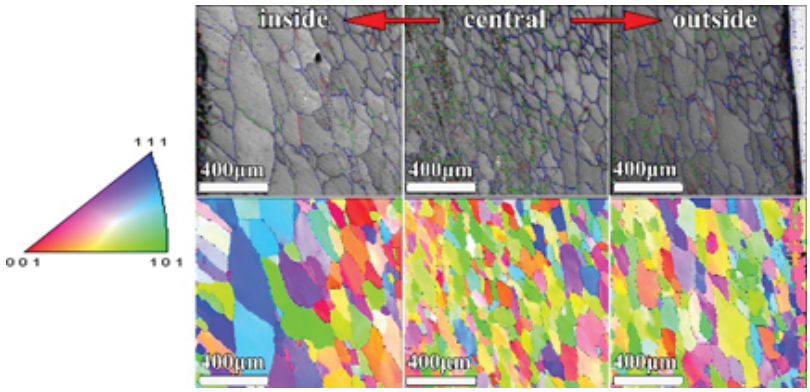

Figure 6: Grain boundary (top) and crystal orientation (bottom) maps in the thickness direction (before deformation).

grains in the thickness direction has been also revealed. The coarse-grain leads to the orange peel defects with a cube texture during deep drawing in st14 steel sheets.

The present study shows that the differences in crystal orientation within a polycrystalline material produce variations in the local yield criteria [9]. The grain rotations by in-situ EBSD measurements have been reported, which allowed studying the amount of rotation and the rotation path of the selected grains. However, the investigation of the changes during tube hydroforming by using in-situ analysis technique presents difficulties. Based on the presented analysis, it is shown that the grain morphology at the surface and its variation along thickness direction, allowing extracting the grain orientation rotation behavior along the tensile load axis, so similar to the data obtained by the in-situ method, can be investigated by the considered method. The grain boundary and orientation maps in the thickness direction are shown in Fig. 7. The pronounced variation of the grain orientation and boundary morphology, which is consistent with the morphology shown in Fig. 6, is observed. In the central area, the grains exhibit low angle boundaries with the angles <15°. However, in the outside and inside areas, part of coarse grains exhibit low misorientation, which indicated that appreciable changes in the local orientation occurred in those grains. At the same time, there still remain a number of the coarse grains with the high angle boundaries. As can be seen from the crystal orientation map, the orientation of central grains demonstrated strong tendency toward <001> orientation, while the layer of 1~4 grains still remains at random orientation. In the inside and outside areas the grains possess low angle boundaries. This can be compared with the grain behavior in the concave areas shown in Fig. 4b. The grain orientation rotation in the central areas inevitably affect the surface grains morphology.

Fig. 8 shows the fraction of the texture in the three areas along the thickness direction before and after tube hydroforming, which corresponds to results shown in Figs. 6 and 7. In all the three areas only [001]<100> Cube and {011}<100> Goss texture components were obtained. It is shown that the volume fraction of the {001}<100> Cube texture component significantly increases in the three areas, especially in the central area (~35%). In contrast, the volume fraction of the {011}<100> Goss decreases in the outside and central areas, but increases slightly in the inside area. This increase of

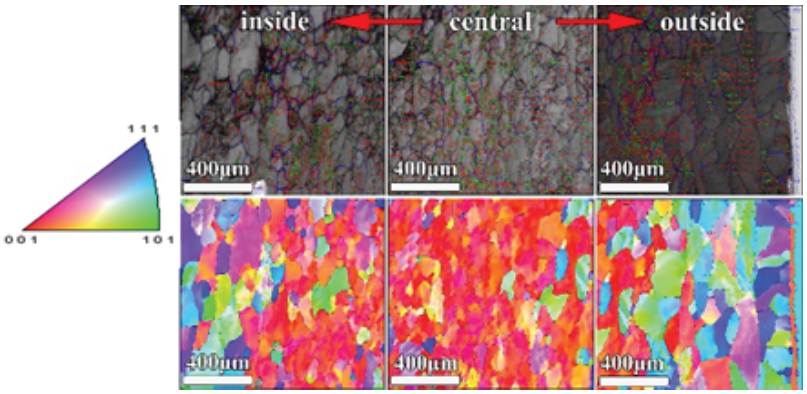

Figure 7: Crystal orientation (top) and grain boundary (bottom) maps in the thickness direction (after tube hydroforming).

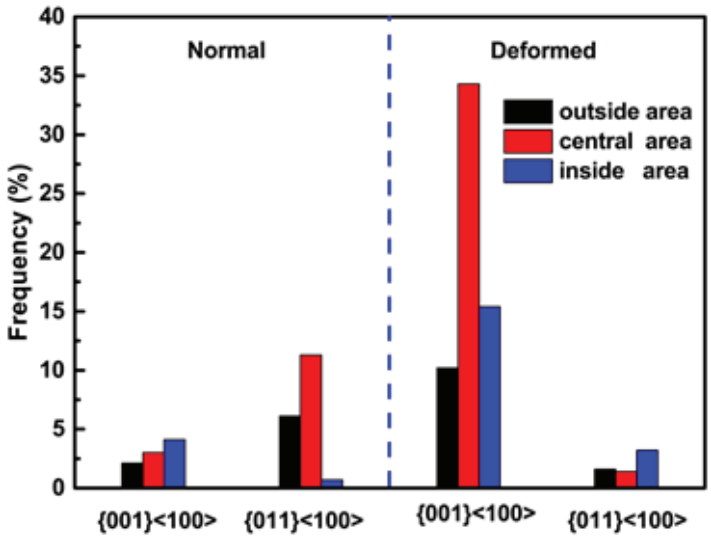

Figure 8: The volume fractions of the texture components in the thickness direction before and after deformation.

volume fraction of the Cube texture occurs, because some grains rotated away from their original orientations, which can cause the rotation of the grains in the marginal areas (inside and outside).

4. Conclusion

Orange peel development in 6063 aluminum alloy tube due to hydroforming was investigated by super depth metallographic microscope and electron backscatter diffraction. It is shown that strong correlation between the surface morphology and the grain boundary and crystal orientation maps exists. This indicates that the surface orange peel phenomena strongly depends on the corresponding grain morphology and grain orientation at the surface and along thickness direction. As regards the surface morphology, a number of grains with low angle boundaries and random orientation were highly deformed and formed the concave areas. The change of the grain orientation tendency from random orientation to <001> orientation in the central

areas along the thickness direction inevitably must influence the change of the outside and inside grains behavior.

References

[1] W. J. Liang, P. A. Rometsch, L. F. Cao, and N. Birbilis, General aspects related to the corrosion of 6xxx series aluminium alloys: Exploring the influence of Mg/Si ratio and Cu, *Corrosion Science*, **76**, 119–128, (2013).

[2] F. Hajializadeh and M. M. Mashhadi, Investigation and numerical analysis of impulsive hydroforming of aluminum 6061-T6 tube, *Journal of Manufacturing Processes*, **20**, 257–273, (2015).

[3] M. R. Stoudt, L. E. Levine, A. Creuziger, and J. B. Hubbard, The fundamental relationships between grain orientation, deformation-induced surface roughness and strain localization in an aluminum alloy, *Materials Science and Engineering A*, **530**, no. 1, 107–116, (2011).

[4] P. D. Wu and D. J. Lloyd, Analysis of surface roughening in AA6111 automotive sheet, *Acta Materialia*, **52**, no. 7, 1785–1798, (2004).

[5] D. Raabe, M. Sachtleber, H. Weiland, G. Scheele, and Z. Zhao, Grain-scale micromechanics of polycrystal surfaces during plastic straining, *Acta Materialia*, **51**, no. 6, 1539–1560, (2003).

[6] P. D. Wu and D. J. Lloyd, Correlation of roping and texture in AA6111 automotive sheet, *Modelling and Simulation in Materials Science and Engineering*, **13**, no. 6, 981–991, (2005).

[7] P. S. Lee, H. R. Piehler, B. L. Adams, G. Jarvis, H. Hampel, and A. D. Rollett, Influence of surface texture on orange peel in aluminum, *Journal of Materials Processing Technology*, **80-81**, 315–319, (1998).

[8] S. Cao, J. Zhang, J. Wu, and J. Chen, Analysis of orange peel defect in St14 steel sheet by electron backscattered diffraction (EBSD), *Journal of Materials Science and Technology*, **21**, no. 1, 17–20, (2005).

[9] S. Kahl, R. L. Peng, M. Calmunger, B. Olsson, and S. Johansson, In situ EBSD during tensile test of aluminum AA3003 sheet, *Micron*, **58**, 15–24, (2014).